Association of Metallurgical Engineers of Serbia *Scientific paper*
AMES *UDC: 620.193/.196:669.711 ; 620.197.3*

THE INHIBITIVE EFFECT OF ETHANOLAMINE ON CORROSION BEHAVIOR OF ALUMINIUM IN NACL SOLUTION SATURATED WITH CO_2

Ivana Jevremović, Vesna Mišković-Stanković*

University of Belgrade, Faculty of Technology and Metallurgy, Karnegijeva 4, 11000 Belgrade, Serbia

Received 11.07.2012
Accepted 24.08.2012

Abstract

In this study, the inhibitive effect of ethanolamine on corrosion behavior of aluminium was investigated in 3 wt. % NaCl solution, saturated with CO_2. All the experiments were carried out at 20°C. Ethanolamine was added at different concentrations between 1 mM and 8 mM. In order to determine the corrosion inhibition efficiency of investigated inhibitor and the optimal concentration of inhibitor that provides the lowest corrosion of aluminium, the open circuit potential (OCP), electrochemical impedance spectroscopy (EIS), linear sweep voltametry (LSV) measurements, weight loss measurements as well as scanning electron microscopy technique (SEM) were performed. The electrochemical study and weight loss measurements indicated that the minimum corrosion rate and maximum inhibition efficiency was detected for concentration of 5 mM of ethanolamine, as well as the ethanolamine did not change the mechanism of aluminium dissolution. The adsorption of ethanolamine was found to obey Frumkin adsorption isotherm at concentrations up to 5 mM, but further increase in concentration was found to deviate from Frumkin adsorption isotherm. The calculated value for interaction parameter a indicates attractive lateral interactions in the adsorbed inhibitor layer. The obtained value of standard free energy of adsorption, ΔG_{ads}^{θ}, confirms that the adsorption process is favorable, spontaneous physisorption process.

Key words: aluminium, corrosion inhibitor, linear sweep voltametry, electrochemical impedance spectroscopy, Frumikin adsorption isotherm, scanning electron microscopy

Introduction

Aluminium is reactive material and prone to corrosion. Its corrosion immunity in various environments can be explained due to the formation of a compact, adherent passive oxide film. When in contact with air or immersed in solution, aluminium is

* Corresponding author: Vesna Mišković-Stanković, vesna@tmf.bg.ac.rs

always spontaneously covered by an oxide film which protects the metal from further oxidation [1]. This surface film is amphoteric and dissolves when exposed to high concentrations of acids or bases [2,3]. Also, the presence of some halogen ions, especially chloride ions, may significantly destabilize the oxide film on aluminium due to its strong dissolution caused by the localized attack [1]. This kind of mechanism has been explained by replacement of water molecules by specifically adsorbed chloride ions at the surface of the dissolving metal [3]. The transfer of metal ions from the metallic phase to the solution can be explained by direct participation of chloride ion in the metal dissolution reaction [4].

Aluminium and aluminium alloys are usually protected from corrosive environments by conversion coatings (phosphate, oxide, chromate, etc.) or some organic-inorganic compounds, and then topcoated with organic coatings, as a barrier layer between the substrate material and the environment [5-7].

Carbon dioxide gas when dissolved in water forms carbonic acid which is corrosive to metals. Injection of film forming inhibitors has been the common method for prevention of CO_2 corrosion. Different groups of organic compounds have been reported to exert inhibitive effects on the corrosion of metals. Most of the inhibitors are organic heterocyclic compounds with N, S, or O atoms [8,9]. The sites of these elements have higher electron density, making them the reaction centers [10]. The addition of corrosion inhibitors effectively secures the metal against an acid attack. It has been found that most of the organic inhibitors act by competitive adsorption on the metal surface with the aggressive ion and by blocking the active corrosion sites [11,12]. The adsorption on the metal surface is influenced by the nature and surface charge of metal, by the type of aggressive electrolyte, and by the chemical structure of inhibitors [13]. Corrosion inhibitors based on organic compounds like alkanolamine influence the corrosion process by forming an adsorptive film on the metal surface [14]. The amino-alcohols are common inhibitors and they are widely applied since they are non toxic and cost attractive [15].

Ethanolamine, commonly called monoethanolamine (MEA) is an organic chemical compound that is both a primary amine and a primary alcohol and acts as a weak base [16]. The main functional groups are hydroxyl and nitrogen atom. All amines have a lone pairs of electrons. However, the readiness with which the lone pair of electrons is available for co-ordination with a proton determines the basic strength of amines [17]. The inhibitive effect of ethanolamine is achieved by donating unshared pair of electrons from nitrogen atom, followed by surface complex forming [18].

In this study the inhibition effect of ethanolamine on the corrosion of aluminium in 3 wt. % NaCl aqueous solution saturated with CO_2 is discussed. In order to determine the corrosion inhibition efficiency of investigated inhibitor and the optimal concentration of inhibitor that provides the lowest corrosion of aluminium, the open circuit potential (OCP), electrochemical impedance spectroscopy (EIS), linear sweep voltametry (LSV) measurements, weight loss measurements and scanning electron microscopy technique (SEM) had been conducted.

Experimental

Electrochemical cell

Experiments were conducted using a conventional three-electrode cell arrangement. The working electrode was pure aluminium panel (10 mm × 10 mm ×

1 mm, purity 99.7 %). The exposed area of the coupon was 1 cm^2. Platinum of 9 mm × 9 mm area was used as counter electrode and saturated calomel electrode as reference electrode. Before being immersed into the electrolyte the working electrode was polished with 600 grit emery papers, degreased with isopropyl alcohol and dried in air. All the experiments were carried out at 20 °C in stagnant conditions. Test solution was 3 wt. % aqueous NaCl, deoxygenated by purging CO_2 gas for 1 h before the start of the experiment and during the whole test in order to maintain positive CO_2 partial pressure and remove dissolved oxygen. The basic inhibition properties of MEA (Fig. 1) on the CO_2 corrosion were investigated by injecting MEA in the solution after the bare aluminium corrosion tests had been conducted. Ethanolamine was added at following concentrations: 1 mM, 3 mM, 4 mM, 5 mM, 7 mM and 8 mM.

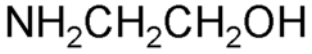

Fig. 1. Molecular structure of the monoethanolamine (MEA)

Electrochemical measurements

All the electrochemical measurements were carried out using Reference 600™ Potentiostat/Galvanostat/ZRA (Gamry Instruments, Inc., Warminster, PA, USA) while the impedance spectra were analyzed using Gamry Instruments Echem Analyst fitting program, version 5.50. Electrochemical impedance spectroscopy (EIS) and linear sweep voltametry (LSV) measurements were performed after 30 min of open circuit potential (OCP) measurements.

The electrochemical impedance measurements were carried out over a frequency range of 10 kHz to 10 mHz using a 10 mV amplitude of sinusoidal voltage variation around the open circuit potential.

The linear sweep voltametry measurements were carried out from a cathodic potential of -200 mV to an anodic potential of +200 mV with respect to open circuit potential with a scan rate of 1 mV/s.

Weight loss measurement

The weight loss was determined by weighing the cleaned samples before and after immersing into the test solution in the absence and presence of ethanolamine at following concentrations: 1 mM, 3 mM, 4 mM, 5 mM, 7 mM and 8 mM. The experiments were carried out in 3 wt. % aqueous NaCl at 20 °C in stagnant conditions. The solutions were deoxygenated by purging CO_2 gas during the whole experiment. After an immersion time of 24 h the cleaning procedure consisted of wiping the coupons with a paper tissue, washing with distilled water and isopropyl alcohol, the sample was then hot air dried and weight.

Characterization of surface morphology

A scanning electron microscope (SEM) JEOL JSM-5800 was used to analyze the morphology of the aluminium surface without and with inhibitor added. Images of the samples were recorded after 24 h exposure time in 3 wt. % aqueous NaCl saturated with CO_2 at 20 °C in stagnant conditions, without and with different concentration of ethanolamine added.

Results and discussion

Open circuit potential measurements (OCP)

The time dependence of the open circuit potential (OCP) was recorded for 30 minutes of immersion of the aluminium specimens in aqueous 3 wt. % NaCl solution saturated with CO_2 without and with ethanolamine added at following concentrations: 1 mM, 3 mM; 4 mM; 5 mM; 7 mM and 8 mM (Fig. 2). A sharp drop in the E_{OCP} was observed after the specimens were immersed in the solution followed by an increase to more positive values. The E_{OCP} reached relatively stationary values after 30 minutes of immersion.

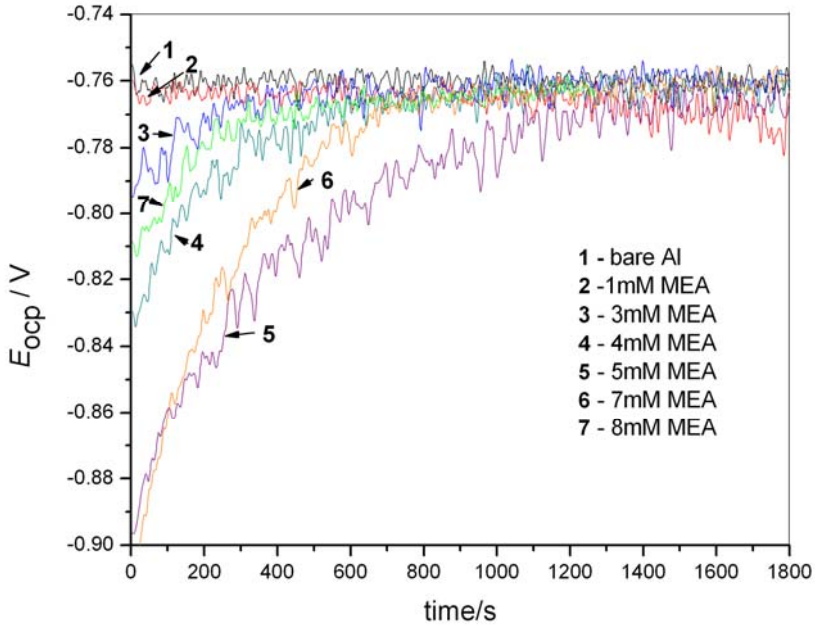

Fig. 2. The time dependence of open circuit potential for aluminium in 3 wt. % NaCl solution saturated with CO_2, at room temperature without and with ethanolamine added at following concentrations: 1 mM, 3 mM; 4 mM; 5 mM; 7 mM and 8 mM.

As it can be seen in Fig.1. the differences in E_{OCP} values are more pronounced at the beginning of the exposure, due to the aggressiveness of the NaCl solution. It was suggested that the initial negative shift would be related to the adsorption of ethanolamine layer on aluminium surface [19]. In the present study these alterations could possibly take place due to the interaction of the ethanolamine molecules with metal surface. The results have shown that the addition of ethanolamine molecules at the beginning shifts E_{OCP} to more negative values, but it should be noted that the stationary values obtained at the end of the exposure time did not show any significant change with addition of inhibitor molecules.

Electrochemical impedance spectroscopy (EIS)

Electrochemical impedance spectroscopy (EIS) was used in order to study the inhibition efficiency of MEA as corrosion inhibitor for aluminium in CO_2 environment. The Nyquist impedance plots of aluminium in 3 wt. % NaCl saturated with CO_2 without and with ethanolamine added at different concentrations are shown in Fig. 3.

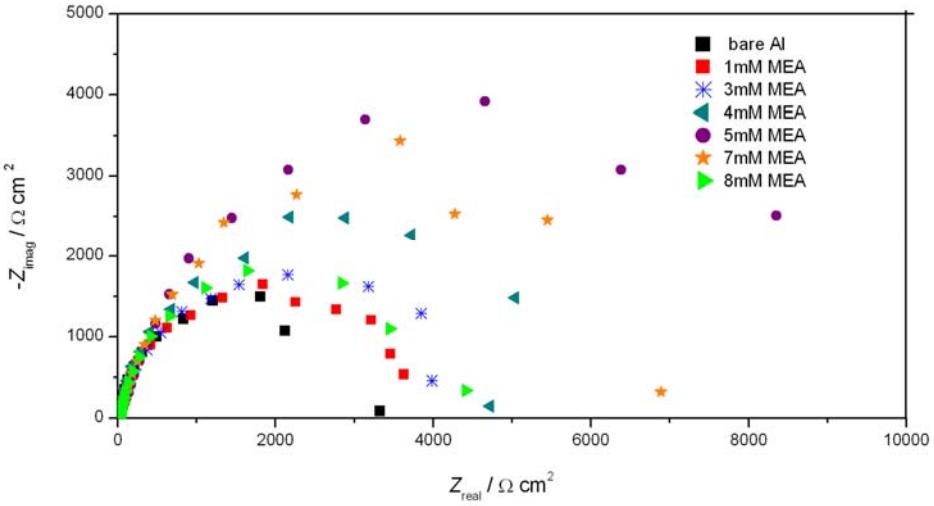

Fig. 3. Nyquist plots of aluminium in 3 wt. % NaCl saturated with CO_2, without and with various concentrations of ethanolamine.

From the Nyquist plots it could be seen that the impedance response changes with the addition of inhibitor molecules. The existence of a single semicircle indicates the presence of simple charge- transfer process during dissolution. The EIS data shows that the presence of ethanolamine increases the values of R_{ct}. Nyquist plots are depressed due to surface roughness, heterogeneity of the surface, or other effects that cause uneven current distributions on the electrode surface [20]. There is no evidence of the formation of a protective oxide or inhibitor film because there is just one capacitive arch in the EIS Nyquist plots but this could be due to the formation of a thin layer of inhibitor film on the aluminium surface with a resistance that is much smaller than the charge transfer resistance.

The EIS data was analyzed using the electrical equivalent circuit represented in Fig. 4, where R_Ω is the solution resistance, R_{ct} is the charge-transfer resistance and *CPE* is the constant phase element, which represents all the frequency dependent electrochemical phenomena, namely double-layer capacitance, C_{dl}, and diffusion processes.

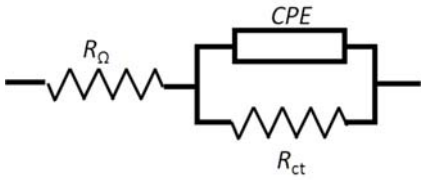

Fig.3. Electric equivalent circuit.

CPE is used in this model to compensate non-homogeneity in the system and is defined by two parameters, Y_0 and n. The impedance of CPE is represented by the following equation [21-23]:

$$Z_{\mathrm{CPE}} = \mathrm{Y}_0^{-1} \cdot (\mathrm{j}\omega)^{-n} \tag{1}$$

where $\mathrm{j} = (-1)^{1/2}$, $\omega = 2\pi f$ is frequency in rad s^{-1}, and f is the frequency in Hz. If n values range from 0.8–1, the impedance of CPE can be considered to be the one of the pure capacitor:

$$Z_{\mathrm{CPE}} = (\mathrm{j}\omega C)^{-\mathrm{n}} \tag{2}$$

and in this case Y_0 gives a pure capacitance (C). The values of charge-transfer resistance obtained from fitting procedure, constant phase element parameter n and double-layer capacitance.

The inhibition efficiency, *IE,* was then calculated using equation (3), where R_{0ct} and R_{ct} are the charge-transfer resistance values without and with inhibitor, respectively. The values of inhibition efficiency are listed in Table 1.

$$IE\% = \frac{R_{ct} - R_{0ct}}{R_{ct}} \cdot 100 \tag{3}$$

Table 1. Corrosion parameters obtained from EIS measurements for aluminium in 3 wt. % NaCl without and with inhibitor MEA.

C_{inh}, mM	R_{ct}, Ωcm^2	*IE*, %	n	$C_{dl}\cdot 10^6$, Fcm^{-2}
blank	3195	-	0.914	60.0
1	3436	7.01	0.891	58.2
3	4452	28.23	0.888	54.8
4	5355	40.36	0.887	66.6
5	11560	72.85	0.852	50.5
7	7938	59.97	0.798	102.1
8	4591	30.40	0.858	100.1

As it can be seen in Table 1 an increase in MEA concentration increases the charge-transfer resistance, R_{ct} values up to 5 mM of ethanolamine due to inhibitor adsorption and then decreases at higher concentrations. The R_{ct} decreases, indicating an increase in the corrosion rate, probably due to desorption of inhibitor. The decrease in double-layer capacitance with increase in MEA concentration up to 5 mM can result from a decrease in local dielectric constant due to the formation of a protective layer on the electrode surface. The thickness of this protective layer increases with increase in inhibitor concentration up to 5 mM, resulting in a decrease in double layer-capacitance. While further increase in inhibitor concentration is followed by double layer-capacitance decrease, probably due to the desorption of inhibitor. These results suggest that MEA molecules function by adsorption at the metal/solution interface.

The values of the inhibition efficiency calculated from impedance measurements for aluminium at different concentrations of ethanolamine in 3 wt. % NaCl saturated with CO_2 are shown in Fig. 5. It has been observed that inhibition efficiency increased with increase in inhibitor concentration and reached a maximum inhibition efficiency of 73 % at a concentration of 5 mM of ethanolamine. The reduction in the dissolution of aluminuim in the presence of tested inhibitor was attributed to the amino group in the inhibitor molecule. This group is electroactive and interacts with the metal surface to a greater extend. Inhibition efficiency then decreases with further increase in inhibitor concentration.

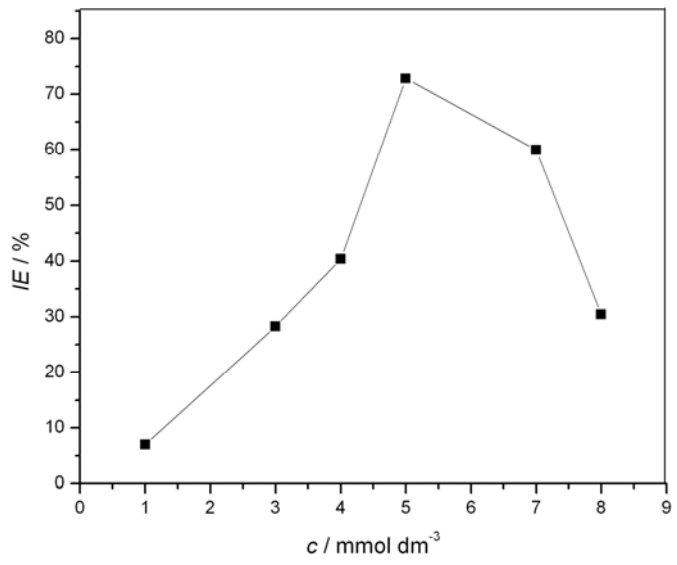

Fig. 5. Dependence of inhibition efficiency, IE, obtained from EIS measurements, on ethanolamine concentrations for aluminium in 3 wt. % NaCl saturated with CO_2.

Fig. 6 represents the Bode plots of aluminium in 3 wt. % NaCl saturated with CO_2, without and with ethanolamine added at different concentrations. The shape of the Bode plots is related to the thickness and the dielectric properties of the film formed on the aluminium electrode. In the high-frequency region the phase angle approaches 0° while in the middle frequency region the capacitive behavior of the system is evident for all concentrations, determined by the dielectric properties of the formed film. In this frequency region phase angle is approaching –90°. As it could be seen in Fig. 6 for inhibitor concentration of 5 mM, besides the peak found around 0 Hz the shoulder at 1000 Hz was observed, indicating the formation of a protective MEA inhibitor film. According to the Bode plots for aluminium in 3 wt. % NaCl solution it can be concluded that 5 mM of ethanolamine added provides good protection to the aluminium surface.

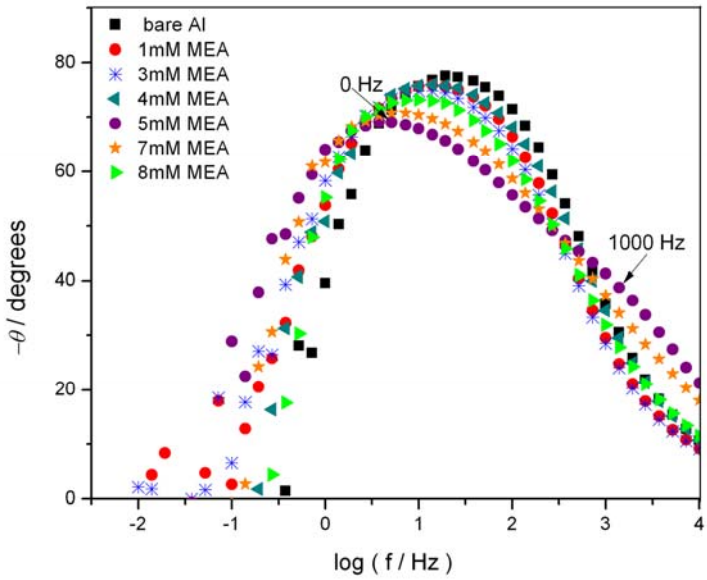

Fig. 6. Bode plots of aluminium in 3 wt. % NaCl saturated with CO_2, without and with various concentrations of ethanolamine.

Linear sweep voltametry (LSV)

The anodic and cathodic polarization curves for the corrosion of aluminium in 3 wt. % NaCl without and with different concentrations of MEA are shown in Fig. 7. The linear Tafel segments of the anodic and cathodic curves were extrapolated to corrosion potential in order to obtain the corrosion current densities (j_{corr}). Corrosion current density, j_{corr} is calculated from the Stern Geary equation (4) where β_a and β_c are anodic and cathodic Tafel slopes, respectively, derived from Tafel curves and R_p is the polarization resistance determined from the slope of the potential versus current density

curve over a narrow potential range from -20 mV to +20 mV relative to the corrosion potential [24].

$$j_{\text{corr}} = \frac{\beta_a.\beta_c}{R_p\, 2.3(\beta_a + \beta_c)} \tag{4}$$

The corrosion kinetic parameters, Tafel constants (β_a and β_c) calculated as slopes of the anodic and cathodic Tafel line, as well as the values of polarization resistance and corrosion current densitiy for aluminium in 3 wt. % NaCl without various concentrations of ethanolamine are given in Table 2. It can be observed from Fig. 7 that increase in ethanolamine concentration shifts the intersecting point of the cathodic and anodic curve (E_{corr}) in the passive (positive) direction. The constant values of Tafel slopes (β_a and β_c), in the presence and absence of inhibitor indicate that there is no change of the mechanism of aluminium dissolution but only the inhibiting action occurred by simple blocking of the available cathodic and anodic sites on aluminium surface. Increase in ethanolamine concentration up to 5 mM decreases the corrosion current density. On the other hand, at concentration higher then 5 mM, the corrosion current density increases, indicating the desorption of inhibitor film. It is shown that results obtained with LSV measurements are in accordance with the EIS measurements.

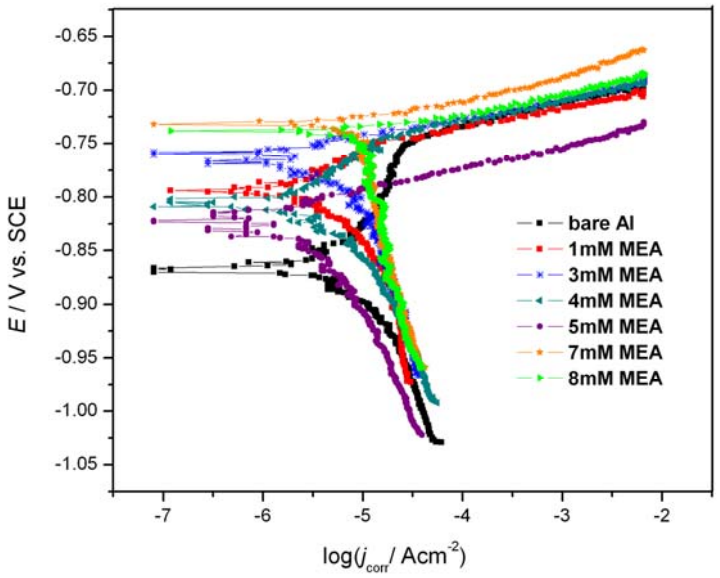

Fig. 7. Polarization curves of aluminium in 3 wt. % NaCl without and with various concentrations of ethanolamine.

Table 2. Corrosion parameters obtained from LSV measurements for aluminium in 3 wt. % NaCl without and with inhibitor MEA after 30 min immersion at open circuit potential.

C_{inh}, mM	R_p, Ωcm^2	β_a, V/dec	β_c, V/dec	$j_{corr}10^5$, Acm^{-2}	*IE*, %
Blank	2585	0.01409	-0.13923	1.178	-
1	3226	0.0431	-0.1247	0.432	19.8
3	3873	0.0135	-0.18612	0.14	33.3
4	5079	0.01491	-0.1219	0.13	49.1
5	9608	0.01915	-0.13931	0.0761	73.1
7	5184	0.02308	-0.3683	0.1935	50.1
8	3269	0.0181	-0.3958	0.2407	26.5

It can be seen from Table 2 that the polarization resistance values increase up to 5 mM and then decrease with higher concentrations of MEA. The cathodic reaction occurring at the aluminium-solution interface is hydrogen evolution. The results show that the cathodic slopes (β_c) are much greater than that expected for H_2 evolution according to Volmer-Tafel mechanism [25]. Such large cathodic Tafel slopes are not unexpected for aluminium, and have previously been reported for H_2 evolution reaction on aluminium electrodes covered probably with an oxide or an oxide-inhibitor complex [26]. The presence of inhibitor film influences the surface reduction process by creating a barrier to charge transfer through the formed film [27].

The dependence of the corrosion current density on inhibitor concentration is shown in Fig. 8.

The corrosion current density decreased with increase in concentration of inhibitor and reached the lowest value of approximately $8 \cdot 10^{-7}$ Acm^{-2} at a concentration of 5 mM of ethanolamine and then increased at higher concentrations of inhibitor. The observed increase in corrosion current density with increase in inhibitor concentration is probably due to the instability of inhibitor film and its desorption from the metal surface. The obtained results are in accordance with inhibition efficiency of ethanolamine (Fig. 5)

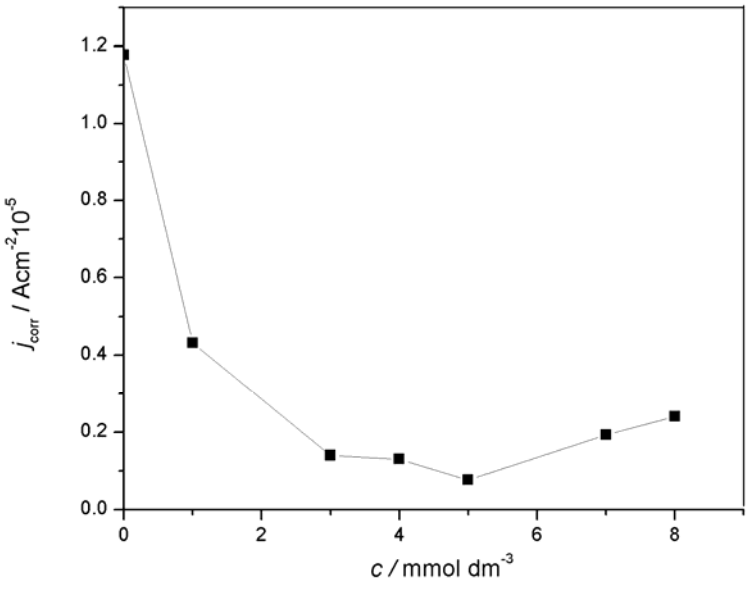

Fig. 8. The dependence of the corrosion current density, j_{corr}, of aluminium in 3 wt. % NaCl without and with various concentration of ethanolamine

Adsorption

The adsorption of organic inhibitors at an electrode/electrolyte interface may take place through displacement of adsorbed water molecules at the inner Helmholtz plane of the electrode, according to the reaction (5) [28]:

$$\text{Ethanolamine}_{(aq)} + n\text{H}_2\text{O}_{ads} = \text{Ethanolamine}_{ads} + n\text{H}_2\text{O}_{(l)} \quad (5)$$

where n is the size ratio, and it represents the number of water molecules displaced by one molecule of organic inhibitor [29]. Aluminium surface is negatively charged in acid solution [30], so protonated ethanolamine molecules can easily approach the negatively charged aluminium surface due to the electrostatic attraction. The inhibitive properties of amines are mainly dependent on the electron densities around the nitrogen atoms; the higher the electron density at the nitrogen atom, the more effective is inhibitor [31,32]. Due to adsorption, inhibitor molecules block the reaction sites and reduce the rate of corrosion reaction [12].

Types of interaction that may occur between ethanolamine and aluminium at the metal–solution interface are electrostatic attraction between charged molecules and the charged metal as well as interaction of unshared electron pair in the molecules with the metal surface [17].

The information on the interaction between the inhibitor and aluminium surface can be provided by the adsorption isotherm. Attempts were made to fit to various

isotherms including Frumkin Langmuir, Temkin, Freundlich, Flory-Huggins, and it was found that the adsorption of ethanolamine follows Frumkin at concentrations up to 5 mM, whereas further increase in concentration of ethanolamine was found to deviate from Frumkin adsorption isotherm (data not shown). Frumkin adsorption isotherm that can be written in the form [33]:

$$\frac{\theta}{1-\theta} = K_{\text{ads}} \cdot c \cdot e^{2a\theta} \tag{6}$$

where θ is the coverage degree, c is the concentration of the inhibitor in the electrolyte, K_{ads} is the equilibrium constant of the adsorption process, and a is an interaction parameter, taking into account the attraction (a > 0) or repulsion (a < 0) between the adsorbed species. For a = 0 (no interaction) this isotherm becomes equivalent to the Langmuir isotherm [34]. The degree of surface coverage (θ) was evaluated from the EIS measurements using equation (7):

$$\theta = \frac{R_{\text{p}} - R_{0\text{p}}}{R_{\text{p}}} \tag{7}$$

where $R_{0\text{p}}$ and R_{p} are the polarization resistance values without and with inhibitor respectively. In order to determine the parameters K_{ads} and a the Frumkin isotherm (4) was linearized in the form:

$$\ln\left(\frac{\theta}{(1-\theta)c}\right) = 2a\theta + \ln K_{\text{ads}} \tag{8}$$

Plot of $\ln\left(\frac{\theta}{(1-\theta)c}\right)$ vs. θ (Frumkin adsorption plot) for the adsorption of ethanolamine on the surface of aluminium in 3 wt. % NaCl saturated with CO_2, without and with ethanolamine is shown in Fig. 9. The obtained plot for Frumkin adsorption isotherm is linear with a correlation coefficient higher than 0.98. The results are indicating that Frumkin adsorption isotherm is valid for concentrations of ethanolamine up to 5 mM.

Frumkin adsorption isotherm consider lateral interactions between adsorbed inhibitor molecules as well as those among inhibitor and water molecules, indicating that the inhibitor is displacing water molecules from the metal surface. The value of the interaction parameter calculated from the slope in the plot representing Frumkin adsorption isotherm (Fig. 9) is a =1.5. The positive sign of the constant a indicates highly attractive lateral interactions in the adsorbed layer [33]. With increasing corrosion inhibitor concentration inhibitor molecules probably start to desorb due to interaction between the inhibiting molecules already adsorbed at the surface and those present in solution. With increasing concentration of the inhibitor, the interactions become stronger, leading to secondary desorption.

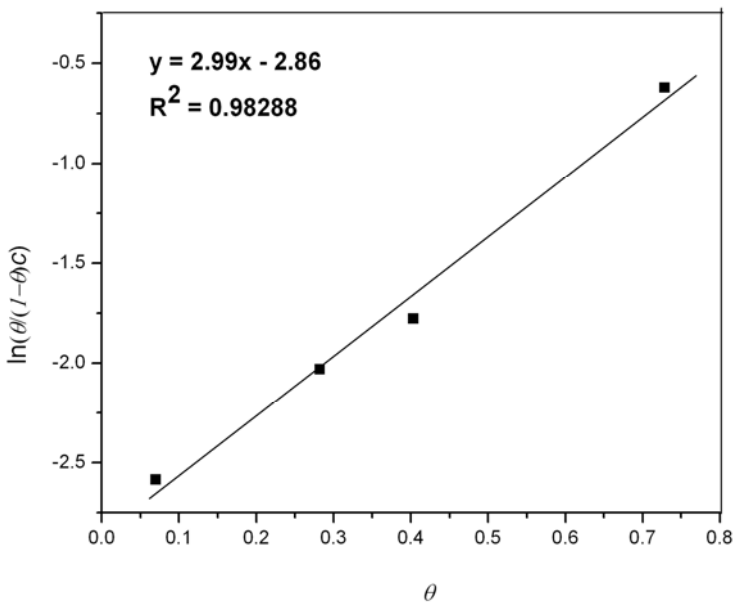

Fig. 9. Frumkin adsorption isotherm at 20°C for aluminium in 3 wt. % NaCl saturated with CO2, in the presence of different concentrations of ethanolamine

Thermodynamic parameters are important to study the inhibitive mechanism. The standard free energy of adsorption ΔG_{ads}^{θ} related to the equilibrium constant of the adsorption process K_{ads} can be obtained from the following equation [28]:

$$K_{ads} = \frac{1}{55.5}\exp\left(\frac{-\Delta G^{o}_{ads}}{RT}\right) \tag{9}$$

where 55.5 is the concentration of water in the solution in 1 mol·dm^{-3}, R the universal gas constant and T the thermodynamic temperature. Calculated value for K_{ads} obtained from the adsorption isotherm intercept is K_{ads} = 0.0573 and acording to the equation (9) standard free energy of adsorption, ΔG_{ads}^{θ} is calculated to be -2.91kJmol^{-1}. The negative value of ΔG_{ads}^{θ} indicates that the inhibitor is spontaneously adsorbed on the aluminium surface [35]. It is generally accepted that the values of ΔG_{ads}^{θ} in aqueous solution up to −20 kJmol^{-1} indicate physisorption. In this type of adsorption the inhibition acts are due to the electrostatic interaction between the charged molecules and the charged metal. While the values of ΔG_{ads}^{θ} around −40 kJmol^{-1} or lower, are seen as chemisorption, which is due to the charge sharing between inhibitor molecules and the metal surface [36]. The obtained value of standard free energy of adsorption, ΔG_{ads}^{θ} in this study is lower then −20 kJ mol^{-1} and it indicates that the adsorption of ethanolamine on aluminium surface represents the pure physisorption.

Weight loss measurement

Weight loss measurement is gravimetric method that was used to estimate inhibition efficiency of ethanolamine and to compare it with results obtained by electrochemical study. The inhibition efficiencies (*IE*%) of different concentration of ethanolamine are also calculated, after an immersion time of 24 h, from the total weight loss by the following equation [37]:

$$IE\% = \frac{WL_0 - WL}{WL_0} \cdot 100 \tag{10}$$

where WL_0 and WL are the weight losses of aluminium without and with the inhibitor added. The values of the inhibition efficiency calculated from weight loss measurements for aluminium in 3 wt. % NaCl at different concentrations of ethanolamine presented in Fig. 10.

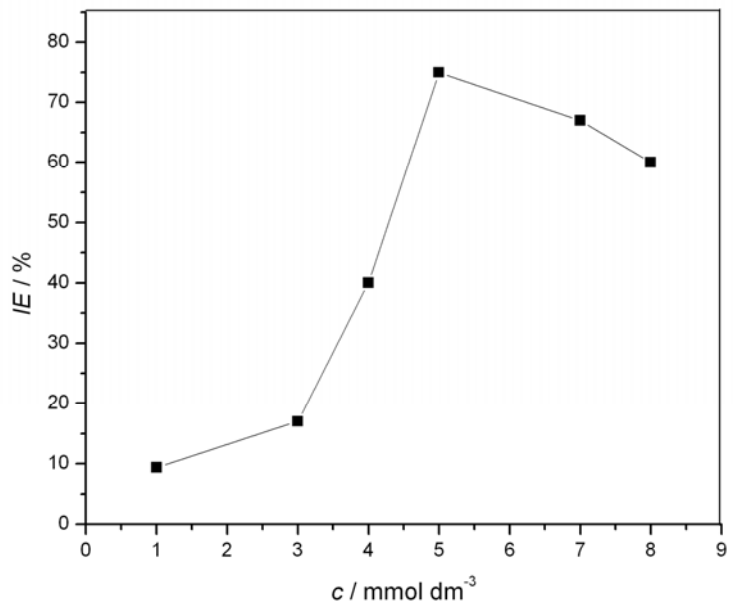

Fig. 10. Dependence of inhibition efficiency, IE, calculated from WL measurements, on ethanolamine concentrations for aluminium in 3 wt. % NaCl saturated with CO_2.

It can be seen from Fig. 10 that inhibition efficiency of ethanolamine reach a maximum value for concentration of 5 mM of ethanolamine, and further increase in inhibitor concentration decreases the inhibition efficiency. It can be noticed that the inhibition efficiency values obtained from weight loss (Fig. 10) and electrochemical measurements (Fig. 5) are comparable. This conclusion is supported by the previously

obtained results that had shown that ethanolamine blocks a fraction of the aluminium electrode reducing the surface area available for corrosion.

Characterization of surface morpology

Fig. 11 shows the aluminum surface after immersion for 24 h in 3 wt. % NaCl without and with ethanolamine added at following concentrations: 1 mM, 5 mM and 7 mM. In the absence of inhibitor (Fig. 11 a) severe damage of aluminium surface is observed. Along the addition of the ethanolamine in test solution (Fig. 11 b-d), the image reveals less roughness, reaching to a uniform surface of aluminium for a concentration of 5 mM of ethanolamine.

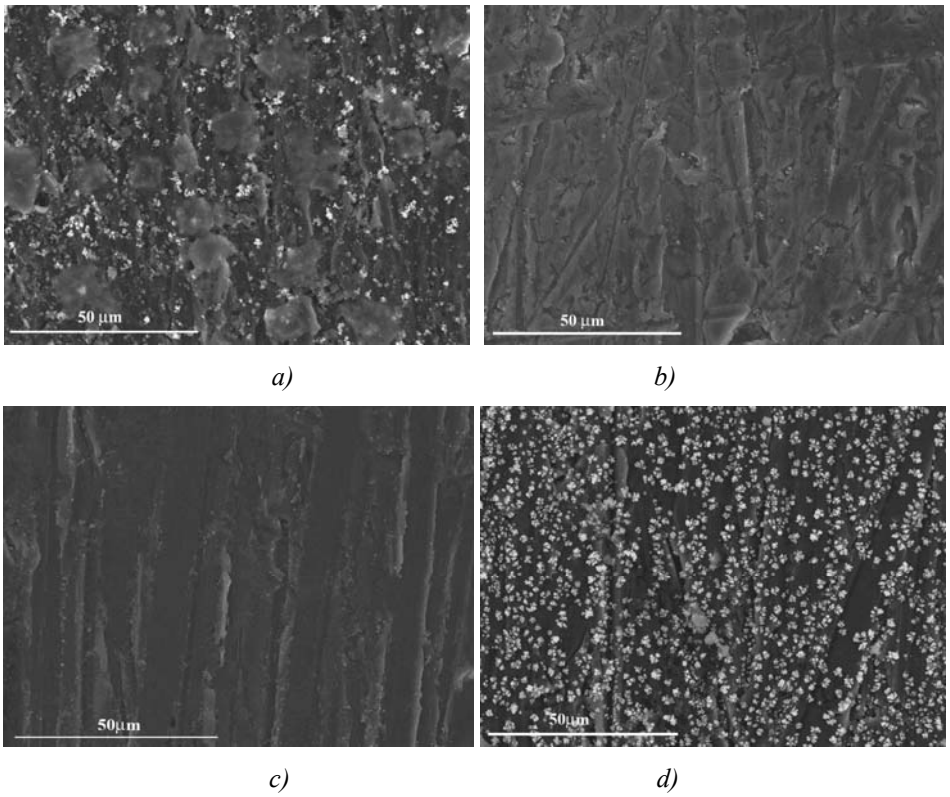

Fig. 11. SEM micrographs of aluminum surface after immersion for 24 h in 3 wt. % NaCl without and with ethanolamine added at following concentrations: (a) bare Al, (b) 1 mM ethanolamine, (c) 5 mM ethanolamine, (d) 7 mM ethanolamine.

The aluminium surface was protected by adsorption of ethanolamine molecules that form a protective film, or due to complex compounds between aluminium and ethanolamine molecules. The micrographs suggest that inhibitor efficiency increases with increasing inhibitor concentration up to 5 mM of ethanolamine and then with increasing inhibitor concentration dissolution of aluminum increases. These results are

supported as well by the electrochemical measurements and weight loss measurement results.

Conclusions

Ethanolamine is found to be good inhibitor for aluminium corrosion in 3 wt. % NaCl saturated with CO_2 with maximum inhibition efficiency around 80 % at a concentration of 5 mM of ethanolamine. Inhibition efficiency is then decreasing at higher concentrations of inhibitor. These results are confirmed by both, electrochemical measurements and weight loss measurements. From the Nyquist plot it can be seen that EIS response indicates the simple charge transfer process during aluminium dissolution. Addition of ethanolamine shifts the corrosion potential slightly in the positive direction without significant change in anodic and cathodic Tafel slopes. This suggests that the inhibition is accomplished by adsorption of ethanolamine molecules on to the aluminium electrode surface without changing the mechanism of partial corrosion reactions. Adsorption of ethanolamine follows Frumkin adsorption isotherm at concentrations up to 5 mM, whereas further increase in concentration of ethanolamine was found to deviate from Frumkin adsorption isotherm. The adsorption of the ethanolamine on aluminium surface is characterized by positive interaction coefficient of the Frumkin isotherm, indicating attractive lateral interactions in the adsorbed inhibitor layer. The negative value of standard free energy of adsorption, ΔG_{ads}^{θ} confirms that the adsorption process is favorable and spontaneous. The obtained value of ΔG_{ads}^{θ} lower than -20 kJ mol^{-1} indicates the pure physisorption process. Corrosion inhibitor concentration higher than 5 mM are probably causing lateral interaction between inhibitor molecules that are leading to inhibitor desorption resulting in the increase in corrosion rate. So it can be concluded that the corrosion of aluminium surface is under control of inhibitor molecules adsorption and desorption process.

Acknowledgements

This research was financed by the Ministry of Education and Science, Republic of Serbia, Grant III 45019.

The authors would like to thank prof. Srđan Nešić, Institute for Corrosion and Multiphase Technology, Ohio University, OH, USA, for helping in discussion of the experimental results.

References

[1] D. Hasenay, M. Seruga, J. Appl. Electrochem. 37 (2007) 1001–1008
[2] X. Li, S. Deng, H. Fu, Corros. Sci. 53 (2011) 2748–2753
[3] R. Ambat, E. S. Dwarkadasa J. Appl. Electrochem. 24 (1994) 911-916
[4] J. J. Heyrovsky, Discussions Faraday Soc. 1 (1947) 212
[5] J.B. Bajat, J.P. Popić, V.B. Mišković-Stanković, Prog. Org. Coat. 69 (2010) 316–321
[6] Z.Ž. Lazarević, V.B. Mišković-Stanković, Z. Kačarević-Popović, D.M. Dražić, Corros. Sci. 47 (2005) 823–834
[7] V.B. Mišković-Stanković, M.R. Stanić, D.M. Drazić, Prog. Org. Coat. 36 (1999) 53-63
[8] S. A. Ali, M.T. Saeed, S.U. Rahman, Corros. Sci. 45 (2003) 253–266
[9] A. Döner, G. Kardas, Corros. Sci. 53 (2011) 4223–423

[10] N. S. Patel, S. Jauhari, G. N. Mehta, Arab. J. Sci. Eng., 34(2009), 61-69
[11] B. Wang, M. Du, J. Zhang, C.J. Gao, Corros. Sci. 53 (2011) 353–361
[12] C. M. A. Brett, I. A. R. Gomes, J. P. S. Martins, Corros. Sci. 36(1994) 915-923
[13] R.A. Prabhu, T.V. Venkatesha, A.V. Shanbhag, G.M. Kulkarni, R.G. Kalkhambkar, Corros. Sci. 50 (2008) 3356–3362
[14] U. Maeder, B. Marazzani, Cement Concrete Comp. 26 (2004) 209–216
[15] L. Be. Mechmeche, L. Dhouibi, M. B. Ouezdou, E. Triki, F. Zucchi, Cement Concrete Comp.30 (2008) 167–173
[16] R. E. Reitmeier, V. Sivertz, H. V. Tartar, J. Amer. Chem. Soc.62 (1940) 1943–1944
[17] C. Jeyaprabha, S. Sathiyanarayanan, G. Venkatachari, Appl. Surf. Sci. 246 (2005) 108–116
[18] R. T. Vashi, H. M. Bhajivala, S .A. Desai, E-J. Chem. 7 (2010), 665-668
[19] L. Kobotiatis, N. Pebere, P. G. Koutsoukos, Corros.Sci. 41 (1999), 941-957
[20] D. Turcio-Ortega, T. Pandiyan, E. M. Garcia-Ochoa, J. Phys. Chem. C 111(2007) 9853-9866
[21] M. Sluyters-Rehbach, Pure Appl. Chem. 66 (1994) 1831-1890
[22] V. D. Jović, B. M. Jović, J. Electroanal. Chem. 541 (2003) 1-11
[23] M.M. Popović, B.N. Grgur, V.B. Mišković–Stanković Prog. Org. Coat. 52 (2005) 359–365
[24] M. Stern, A. L. Geary, J. Electrochem. Soc. 104 (1957) 56-63
[25] J. O'M. Bockris, A. K. N. Reddy, M. Gamboa-Aldeco, Modern Electrochemistry, second ed., Kluwer Academic/ Plenum Publishers, New York, 2000, 862- 910
[26] M. A. A. Rahim, A. A. A. Rahman, M. W. Khalil, Materialwiss. Werkst. 27(1996) 438-443
[27] E. A.Abd El-Wahab, A.H. Marei, O. R.Khalifa, H.A. Mohamed, J. Amer. Sci. 8 (2010) 476-478
[28] S. Zhang, Z. Tao, S. Liao, F. Wu, Corros. Sci. 52 (2010) 3126–3132
[29] M.A. Quraishi, S. K. Shukla, Mater. Chem. Phys. 113 (2009) 685–689
[30] A. S. Fouda, G. Y. Elewady A. El-Askalany, K. Shalabi, Zaštita materiala, 51 (2010) 206- 219
[31] H. Ju, Z. P. Kai, Y. Li, Corros. Sci. 50 (2008) 865–871
[32] A. Yurt, S. Ulutas, H. Dal, Appl. Surf. Sci. 253 (2006) 919
[33] Lj. M. Vracar, D.M. Drazic, Corros. Sci. 44 (2002) 1669–1680
[34] M. Christov , A. Popova, Corros. Sci. 46 (2004) 1613–1620
[35] A.S. Fouda, M. Abdallah, I.S. Ahmed, M. Eissa, Arab. J. Chem. (2010) article in press
[36] K.F. Khaled, M.M. Al-Qahtani, Mater. Chem. Phys. 113 (2009) 150–158
[37] M. A. Amin, S. S. A. EI-Rehim, E.E.F. El-Sherbini, O. A. Hazzazi, M. N. Abbas, Corros. Sci. 51 (2009) 658–667.